Rare Metal Materials and Engineering
Volume 47, Issue 4, April 2018
Online English edition of the Chinese language journal

Available online at www.sciencedirect.com
ScienceDirect

Cite this article as: Rare Metal Materials and Engineering, 2018, 47(4): 1043-1048.

ARTICLE

Ablation Resistance of APS Sprayed Mullite/ZrB_2-$MoSi_2$ Coating for Carbon/Carbon Composites

Han Wei[1,2], Liu Min[2], Deng Chunming[2], Liu Xuezhang[2], Zeng Dechang[1], Zhou Kesong[2]

[1] South China University of Technology, Guangzhou 510640, China; [2] Guangdong Provincial Key Lab for Modern Materials Surface Engineering Technology, National Engineering Laboratory for Modern Materials surface Engineering Technology, Guangdong Institute of New Materials, Guangzhou 510650, China

Abstract: Mullite/ZrB_2-$MoSi_2$ coating was deposited on carbon/carbon(C/C) composites to protect against ablation by atmospheric plasma spraying (APS). The microstructure and morphology of the coating were characterized by X-ray diffraction, scanning electron microscopy and energy dispersive spectroscopy. The ablation resistance of the coating was investigated at different temperatures with oxypropylene torch. The results show that the mass ablation rates of the Mullite/ZrB_2-$MoSi_2$ coated C/C composites are 3.49×10^{-3} g/s and 3.77×10^{-3} g/s after ablation at 1700 and 1800 °C for 60 s, respectively, which exhibit good ablation resistance compared with the single-layer ZrB_2-$MoSi_2$ coated. The increase of ablation resistance can be attributed to the formation of a silicates glass film, which acts as a thermal barrier and self-seals the defects of the coatings.

Key words: C/C composites; atmospheric plasma spraying; coating; ablation

Carbon/carbon (C/C) composites are very promising structural materials which can keep great mechanical properties at high temperature above 2000 °C[1]. Recently, C/C composites have been widely applied to space vehicles and turbine engines for their outstanding properties, such as high strength-to-weight ratio and excellent thermal shock resistance[2,3]. Nevertheless, the poor ablation resistance in the oxygen-containing atmosphere at the ultra-high temperature plume with high-speed gas flow becomes a fatal weakness to their applications. Ceramic coatings have been approved to be an effective method to protect C/C composites from ablation[4-6].

Among the ultra-high temperature ceramic (UHTC) coatings, ZrB_2-based coating, which has extremely high melting temperature and superior thermal conductivity, has been considered as one of the most attractive materials for thermal protection system[7-9]. Furthermore, SiC and $MoSi_2$ are introduced into ZrB_2 coating to improve its ablation resistance due to the formation of SiO_2 glass with self-sealing ability at high temperature[10,11]. But, the viscosity of SiO_2 glass will decline when ablation temperature exceeds 1650 °C, which leads to the rapid volatilization of SiO_2 glass and a single ZrB_2-based coating fails to provide long-term protection for C/C composites at elevated temperature[12]. Then, multilayer coatings have attracted much attention for anti-ablation of C/C composites. A lot of multilayer coatings such as ZrB_2-$CrSi_2$-Si/SiC, $ZrSiO_4$/SiC and $MoSi_2$-SiC-TaC have been reported[13-15].

Mullite ($3Al_2O_3{\cdot}2SiO_2$) coating has applied widely as environmental barrier coating (EBC) for its high thermal and chemical stability, lower oxygen permeability, good erosion resistance associated with the sealing properties of silica[16,17]. Up to now, mullite coatings were prepared by sol-gel[18], CVD[19], and supersonic plasma spraying[20] for SiC-coated C/C composites, and they all exhibited remarkable oxidation protection ability in static air under ambient pressure below 1500 °C. But little research had been conducted on the ablation behavior of mullite in an erosive environment with ultra-high temperature, high pressure and high velocity of combustion gas flow.

Received date: April 25, 2017
Foundation item: Provincial Natural Science Foundation of Guangdong Province (2016A030312015); Guangdong Science and Technology Program (2013B050800031, 2014B050502008, 2015B070701024)
Corresponding author: Liu Min, Ph. D., Professor, Guangdong Institute of New Materials, Guangzhou 510650, P. R. China, Tel: 0086-20-37238263, E-mail: liumin_gz@163.net

In the present work, multilayer mullite/ZrB_2-$MoSi_2$ coating was deposited on C/C composites by atmospheric plasma spraying (APS) technique. The ablation resistance of the coated C/C composite was investigated by oxypropylene torch test and the microstructures and phase compositions of the mullite/ZrB_2-$MoSi_2$ coating after ablation were also discussed.

1 Experiment

Bulk C/C composites with a density of 1.70 g/cm^3 were cut into small specimens (Φ30 mm×20 mm) to be used as substrates. The specimens were hand-polished using SiC paper, then cleaned ultrasonically with ethanol and dried in air. The mixture of 60 wt% ZrB_2 and 40 wt% $MoSi_2$ powders (Eno Material Co. Ltd. China) was manufactured by means of ball milling, spray drying and thermal treatment in turn to ensure good flowability and intensity of particles. Mullite powder with a particle size in the range 45~75 μm was purchased from Beijing Sunspraying Technology Co. Ltd. China. Mullite/ZrB_2-$MoSi_2$ (M/ZM) coatings were deposited on the C/C substrate using a plasma spray system (MF-P1000, GTV, Germany). The detailed parameters are listed in Table 1. While, the single-layer ZrB_2-$MoSi_2$ (ZM) coating with a thickness of about 200 μm was deposited as a control.

The ablation test of coated samples was carried out under oxypropylene torch system. The experimental ablation set-up and practical image (Oriental Renpro Technologies Co. Ltd. China) are shown in Fig.1. The oxypropylene gun tip has seven same symmetric distribution nozzles with inner diameter of 2 mm. The sample was placed in a graphite concave fixture and exposed to the flame vertically with estimated temperature for 60 s. The surface and back-face temperature of the samples were measured by an infrared pyrometer and a thermocouple, respectively. The distance between gun tip and sample surface was 30 mm. The mass ablation rates were calculated by the mass change of the samples before and after ablation test. Compared with a traditional ablation test, the condition of ablation test in the paper was more rigorous. The details of ablation test can be found in Table 2.

The phase composition and morphology of the coated composites were analyzed by X-ray diffraction (XRD, D8-Advance, Bruker) and scanning electron microscopy (FE-SEM, Nova-Nona-430, FEI) equipped with energy dispersion spectroscopy (EDS).

2 Results and Discussion

2.1 Phase composition and microstructure

Fig.2a shows the surface SEM morphology of the ZM inner coating deposited by the first step of APS. It is obvious that the surface is rugged and rough, which is beneficial for the mechanical bonding of the following mullite coating. The corresponding XRD pattern can be found in Fig.2b. It reveals that the inner coating is mainly composed of ZrB_2, $MoSi_2$ and ZrO_2. The oxidation of part $MoSi_2$ at temperature above 1000 °C leads to the formation of Mo_5Si_3 phase[21].

Another mullite coating was then deposited on the ZM inner coating by the second step of APS with the parameters listed in Table 1. Fig.3a displays the SEM images of the coated mullite. The surface of the coating exhibits a homogeneity structure without crack, as well as a low porosity. It is well known that good melting degree, narrow size distribution and high kinetic energy of feedstock particles can all reduce porosity. As shown in Fig.3b, the multilayer coating exhibits typical two-layer structure: the outer mullite layer (60~80 μm) and inner ZrB_2-$MoSi_2$ layer (100~120 μm).

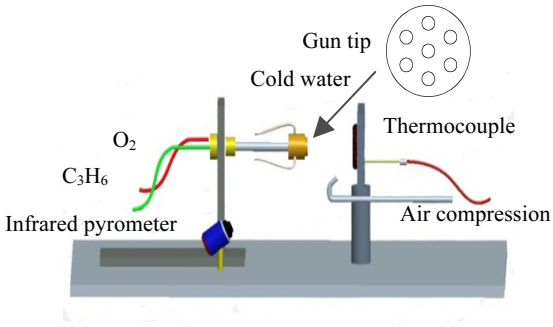

Fig.1 Oxypropylene torch system for measuring ablation resistance of the coated specimen

Table 1 Details of plasma spraying parameters for ZrB_2-$MoSi_2$ and mullite coatings

Coating	Spraying current/A	Spraying voltage/V	Primary gas Ar/L·min^{-1}	Second gas H_2/L·min^{-1}	Powder feed rate/g·min^{-1}	Spraying distance/mm
ZrB_2-$MoSi_2$	700	75	40	11	7	110
Mullite	630	69	40	11	8	100

Table 2 Details of ablation test

Samples	Flux of C_3H_6/ L·min^{-1}	Flux of O_2/ L·min^{-1}	Surface temperature/°C	Ablation time/s	Mass ablation rate/×10^{-3} g·s^{-1}
1# (ZM)	7	31	1700	60	6.38
2# (M/ZM)	7	30	1700	60	3.49
3# (ZM)	8	35	1800	60	8.63
4# (M/ZM)	8	34	1800	60	3.77

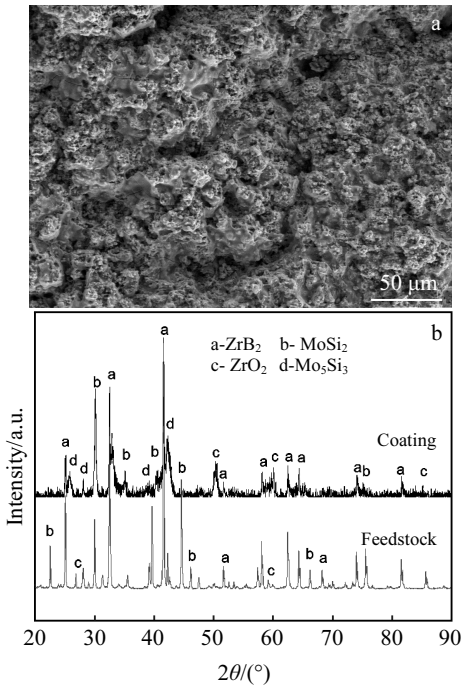

Fig.2 SEM morphology of ZrB_2-$MoSi_2$ coating (a) and XRD patterns of the ZrB_2-$MoSi_2$ feedstock and the coating (b)

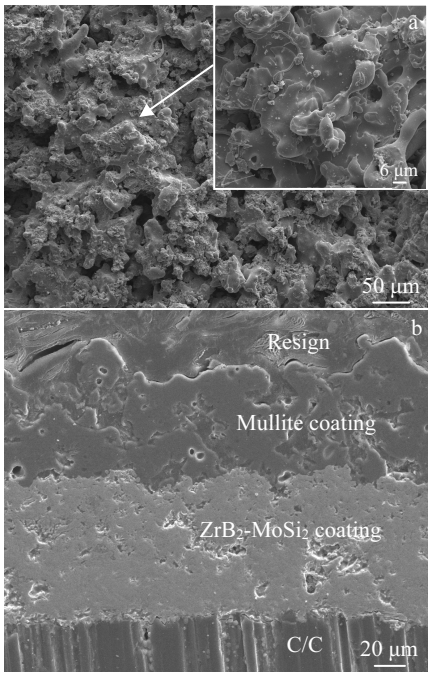

Fig.3 SEM images of surface (a) and cross-section (b) of mullite coating

Moreover, an interlock structure without obvious penetration crack can be found between inner ZM layer and outer mullite layer, which indicates perfect interface bonding. Fig.4 shows the XRD patterns of mullite feedstock and as-sprayed

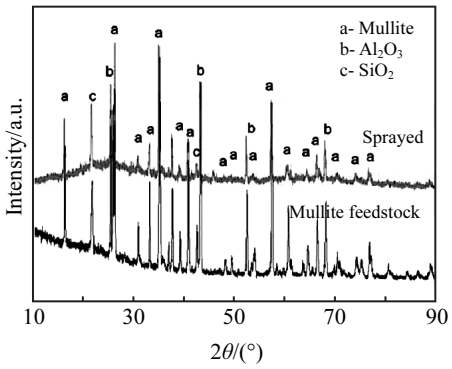

Fig.4 XRD patterns mullite feedstock (a) and as-sprayed (b) coating

coating. They are both mainly composed of orthorhombic $3Al_2O_3$-$2SiO_2$ mullite and a small amount of Al_2O_3 and SiO_2. While, there is a broad hump at low 2θ angles, which indicates that an amorphous glassy phase is present in the as-sprayed coating. During atmospheric plasma spraying process, the rapid quenching rate of molten droplets of mullite feedstock can result in amorphous phase.

2.2 Ablation resistance of the coating

The ablation results of the single layer and multilayer coating specimen are listed in Table 2. When the surface temperature at ablation center of coated sample comes to 1700 °C, the mass ablation rates of 2# sample is 3.49×10^{-3} g/s after ablation duration of 60 s, which is reduced by 45% compared with 1# sample. With the increase of heat flux, the mass ablation rates of both samples increase. The mass ablation rate of 4# sample is 3.77×10^{-3} g/s after ablation for 60 s at 1800 °C, while 3# sample is 8.63×10^{-3} g/s.

Fig.5 presents the macrographs of the C/C sample with single ZM coating and multilayer M/ZM coating after ablation for 60 s. As shown in Fig.5a, there are a great quantity of yellow porous films which are formed and diffusely distributed in the ablation center of 1# sample, and part of them crack and peel from the sample surface. In Fig.5b, the M/ZM coating of 2# sample keeps relatively complete and the surface is still uniform. Three distinct ablation regions (central ablation region, transitional ablation region and outer ablation region) can be distinguished out depending on surface color and ablation morphology. In Fig.5c, the ablation holes are visible at the ablation center of 3# sample. It results in the direct exposure of C/C composite under the oxypropylene flame, which implies that the single ZM coating loses its protective ability as the ablation temperature increases up to 1800 °C. The central region of 4# sample shows deep pits, but the coating is still integrated in border region (Fig.5d).

Fig.6 represents XRD patterns of the 1# and 2# coated C/C samples after ablation for 60 s. The phases of 1# sample are mainly ZrO_2 and SiO_2. During ablation test, ZrB_2, $MoSi_2$ and Mo_5Si_3 are oxidized to form ZrO_2, SiO_2, B_2O_3 and MoO_3.

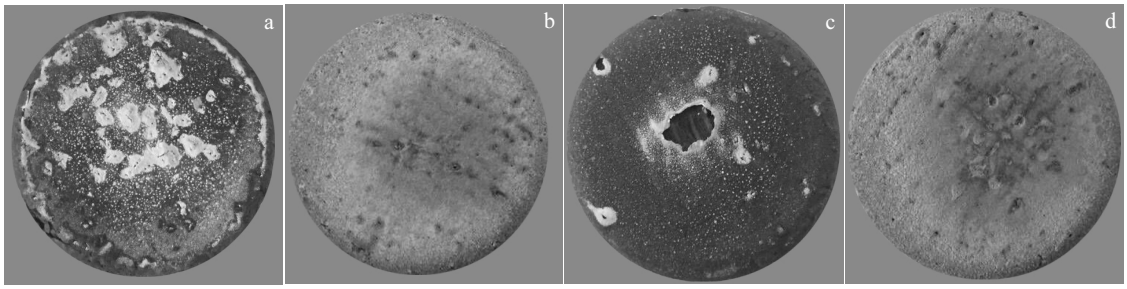

Fig.5 Morphologies of different coated C/C composites after ablation for 60 s under different heat fluxes with the oxypropylene flame: (a) 1# ZM coating, (b) 2# M/ZM coating, (c) 3# ZM coating, and (d) 4# M/ZM coating

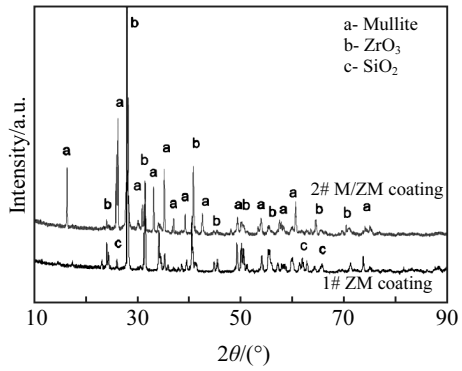

Fig.6 XRD patterns of different coated C/C composites after ablation for 60 s under the oxypropylene flame

The coating of 2# sample is mainly composed of crystalline mullite phase (ZrO_2 phase is a minor phase), whereas Al_2O_3 and SiO_2 peaks disappear in the M/ZM coating after ablation, suggesting a reaction between free alumina and silica during ablation test.

Fig.7a shows the surface SEM morphology of ablation center region of 2# sample. The uniform surface with ablation pits is observed from the M/ZM coating in center region, in which some wire-shape mullite crystals with the size of 2~3 μm could be distinguished as well. It is the quick cooling of the sample that induces the formation of little cracks. From the cross-sectional morphologies of the coatings (Fig.7b), inner ZM coating can be divided obviously into three layers (e.g. as-sprayed layer, transitional layer, loose layer). Some micropores can be found on the loose layer, which might be attributed to the escape of SiO and B_2O_3 generated from the oxidation of ZM inner coating as the ablation temperature is up to 1700 °C. However, the formation of SiO_2 glass as a buffering layer will gradually seal the pores of ZM inner layer and mullite outer layer, which has contributed to the appearance of a dense mullite outer layer. There are two major reasons for this phenomenon. Firstly, there are complex relations between glass composition and viscosity. In general, the viscosity of SiO_2 glass increases with enhancement of the

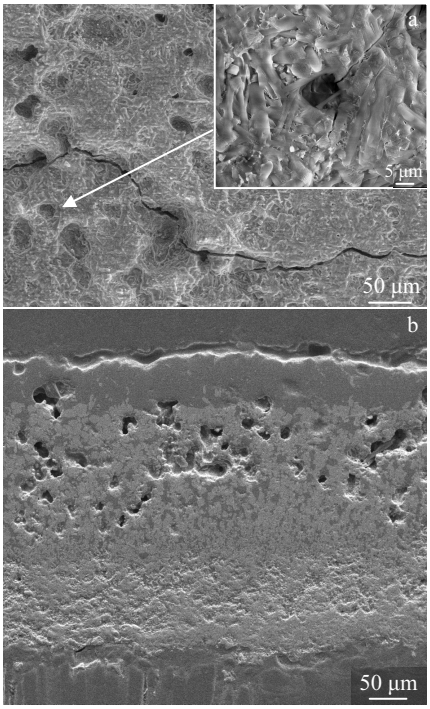

Fig.7 SEM morphologies of surface (a) and cross-section (b) for the M/ZM coating of 2# sample after ablation in center region

cation bond strength in the same condition, and the introduction of mullite may improve the viscosity of SiO_2 glass. Secondly, mullite layer is a good thermal barrier, which could hinder the heat transfer and gas flow. Therefore, the less glass may be evaporated in the short ablation time.

Fig.8 shows the SEM morphology of 4# sample in center region after ablation for 60 s. When the surface temperature of specimen is up to 1800 °C, part of the ablation products in the ablation center are blown away by the gas flow. Two primary reasons for the phenomenon can be deduced. Firstly, the shearing force of the oxypropylene flame during ablation increases with the increase of gas flow rate. Secondly, the viscosity of SiO_2 glass decreases with the temperature increasing, which can result in the formation of more pores and cracks in the coating. As shown in the enlarged image

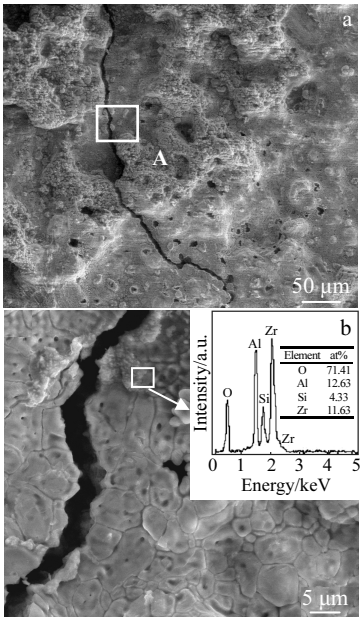

Fig.8 SEM morphologies of low (a) and high (b) magnification and EDS analysis of 2# sample after ablation in center region

(Fig.8b), the width of microcrack is about 3 μm. According to the EDS result, the molten products near the microcrack are composed of ZrO_2 and mullite. The ablation temperature is close to the melting point (1850 °C) of mullite, which may lead to the formation of liquid phase. Then ablation pores and microcracks are filled with liquid mullite, which can reduce inward diffusion of oxygen and exhibit good ablation resistance. Without protection of mullite coating, the SiO_2 glass would be consumed quickly that results in the formation of many pores and cracks in the single ZrB_2-$MoSi_2$ coating. Oxygen can diffuse through the coating and directly attack the C/C composite by the defects in the ZrB_2-$MoSi_2$ layer. With ablation time extending, the coating would be debonded gradually by the high-speed gas flow of oxypropylene flame, leading to the degradation of the protective ability of the coating.

Fig.9 shows the schematic diagram of mullite/ZrB_2-$MoSi_2$ coating ablated with the oxypropylene flame. During the ablation test, the following reactions could take place[22]:

$$2ZrB_2(s) + 5O_2(g) = 2ZrO_2(s) + 2B_2O_3(g) \quad (1)$$

$$2MoSi_2(s) + 7O_2 = 2MoO_3(g) + 4SiO_2(l) \quad (2)$$

$$SiO_2(s) + 3Al_2O_3{\cdot}2SiO_2(s) = \text{Silicates glass (m)} \quad (3)$$

$$\text{Silicates glass (m)} = Al_2O_3 + SiO_2(s) \quad (4)$$

In the initial stage of ablation, oxygen can diffuse into the interface between ZM inner layer and mullite outer layer through the microcracks and voids of the mullite coating, which will result in the oxidation of ZrB_2 and $MoSi_2$ and the formation of ZrO_2, B_2O_3, MoO_3 and SiO_2 (Eqs.(1) and (2)). When the surface temperature of the specimen reaches to 1700 °C, the porous structure would be formed with the evaporation of B_2O_3, MoO_3 and SiO_2. Part of SiO_2 may gradually seal the

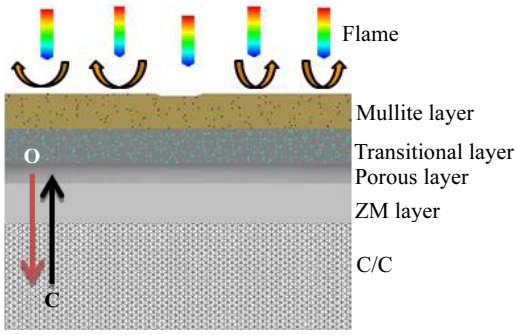

Fig.9 Schematic diagram of the ablated coating under the oxypropylene flame

ZM inner layer and mullite layer. As a result, the mullite layer could be gradually dissolved into coating. The thicker silicates glass can be formed with the dissolution of the mullite layer, which will act as a thermal barrier and improve the ablation resistance of the coating due to the low oxygen permeation constant and good self-cure ability. In general, the chemical erosion is the main ablation behavior of the coating under the low heat flux. With the heat flux of oxypropylene flame increasing, the quick volatilization of the glass film (Eq.(4)) may lead to the further diffusion of oxygen through the formed defects and the decrease in coating thickness. What is more, the silicates glass would be blown away by the high-velocity and high-temperature gas flow gradually due to the severe mechanical denudation.

3 Conclusions

1) A mullite/ZrB_2-$MoSi_2$ coating is prepared on C/C composites by atmospheric plasma spraying.

2) This multilayer mullite/ZrB_2-$MoSi_2$ coating exhibits better ablation resistance at 1700 and 1800 °C compared with single ZrB_2-$MoSi_2$ coating, which contributes to the formation of silicates glass acting as a thermal barrier to oxidation and mechanical erosion.

3) With the increase of heat flux, the failure of the multilayer coating is attributed to the consumption of the glass film due to the increase of chemical erosion and mechanical denudation.

References

1 Sheehan J E, Buesking K W, Sullivan B J. *Annual Review of Materials Science*[J], 2003, 24: 19

2 Krenkel W, Berndt F. *Materials Science and Engineering A*[J], 2005, 412: 177

3 Vignoles G L, Aspa Y, Quintard M. *Composites Science and Technology*[J], 2010, 70: 1303

4 Wang Y J, Li H J, Fu Q G *et al*. *Ceramics International*[J], 2013, 39: 359

5 Singh M, Jessen T. *Carbon*[J], 2002, 40: 583

6 Corral E L, Walker L S. *Journal of the European Ceramic Society*[J], 2010, 30: 2357
7 Wang Z, Wang S, Zhang X *et al*. *Journal of Alloys and Compounds*[J], 2009, 484: 390
8 Yang X, Wei L, Song W *et al*. *Composites: Part B Engineering*[J], 2013, 45: 1391
9 Monteverde F, Bellosi A. *Journal of the Electrochemical Society*[J], 2003, 150: B552
10 Huang D, Zhang M Y, Huang Q Z *et al*. *Transactions of Nonferrous Metals Society of China*[J], 2015, 25: 3708
11 Karlsdottir S N, Halloran J W. *Journal of the American Ceramic Society*[J], 2007, 90: 3233
12 Zhang Y L, Hu Z X, Li H J *et al*. *Ceramics International*[J], 2014, 40: 14 749
13 Feng T, Li H J, Hu M H *et al*. *Journal of Alloys and Compounds*[J], 2016, 662: 302
14 Liu J, Cao L Y, Huang J F. *Surface & Coatings Technology*[J], 2012, 206: 3270
15 Pu H, Niu Y R, Hu C *et al*. *Ceramics International*[J], 2015, 41: 11 387
16 Varadarajan S, Pattanaik A K, Sarin V K. *Surface & Coatings Technology*[J], 2001, 139: 153
17 Fritze H, Jojic J, Witke T *et al*. *Journal of the European Ceramic Society*[J], 1998, 18: 2351
18 Wen Z L, Xiao P, Li Z *et al*. *Journal of the European Ceramic Society*[J], 2015, 35: 3789
19 Wang K T, Cao L Y, Huang J F *et al*. *Journal of the European Ceramic Society*[J], 2013, 33: 191
20 Ma C, Li H J, Wu H *et al*. *Journal of Materials Science and Technology*[J], 2013, 29: 29
21 Natesan K, Deevi S C. *Intermetallics*[J], 2000, 8: 1147
22 Wu H, Li H J, Fu Q G *et al*. *Journal of Thermal Spray Technology* [J], 2011, 20: 1286

C/C 复合材料大气等离子喷涂 mullite/ZrB_2-$MoSi_2$ 涂层抗烧蚀性能

韩　伟[1,2]，刘　敏[2]，邓春明[2]，刘学璋[2]，曾德长[1]，周克崧[2]

(1. 华南理工大学，广东 广州 510640)

(2. 广东省新材料研究所 现代材料表面工程技术国家工程实验室 广东省现代材料表面工程重点实验室，广东 广州 510650)

摘　要：采用大气等离子喷涂技术(APS)在 C/C 复合材料表面制备了 mullite/ZrB_2−$MoSi_2$ 双层抗烧蚀涂层。借助 XRD、SEM、EDS 等分析手段对涂层的组织结构进行研究；基于氧丙烯焰烧蚀试验考察 ZrB_2−$MoSi_2$/mullite 复合涂层对 C/C 复合材料高温耐烧蚀性能的影响。结果表明，在 1700 和 1800 ℃的氧丙烯焰下烧蚀 60 s，ZrB_2−$MoSi_2$/mullite 涂层试样的质量烧蚀率分别为 3.49×10^{-3} 与 3.77×10^{-3} g/s。其与单层 ZrB_2-$MoSi_2$ 涂层试样相比，ZrB_2-$MoSi_2$ /mullite 涂层试样展现了出色的抗烧蚀性能。烧蚀过程中形成的硅酸盐玻璃可以作为热障层而减少氧气的进一步渗透，并且还具有自我封填缺陷的能力，使 ZrB_2-$MoSi_2$/mullite 涂层表现较好的抗烧蚀性。

关键词：C/C 复合材料；等离子喷涂；涂层；烧蚀

作者简介：韩　伟，男，1992 年生，硕士生，华南理工大学材料科学与工程学院，广州 510640，电话：020-37238263，E-mail: weihan_hg@163.com